MULTI-DISCIPLINARY DESIGN OPTIMIZATION OF A BLENDED WINGLET

Joabe Marcos de Souza*, Fernando Martini Catalano*
***University of São Paulo – São Carlos Engineering School – São Paulo - Brazil**

Keywords: *MDO, VLM, blended winglet, optimization, commuter aircraft*

Abstract

In order to reduce operating costs directly related to fuel burn, it is proposed the development of a blended winglet optimized for a commuter aircraft of 11 passengers. Initially a brief description of the problem is made, as well as the background of the wingtip devices evolution. The optimization method used to model the physical phenomena in question, the drag generated by lift, was a Vortex Lattice Method (VLM) code based on the Trefftz-Plane theory for counting induced drag. After the iterative process the results are analyzed, presenting the comparisons between the aircraft without / with the final winglet. These comparisons cover several areas of aeronautics, such as aerodynamics, loads and performance.

1 Introduction

The category of aircraft proposed for the winglet optimization was a commuter aircraft up to 19 passengers meeting the requirements of the 14 CFR Part 23 regulations. After a dense data analysis, the design was directed to the aircraft with the lowest operational cost. As result, the aircraft ABQ11 (Fig. 1) was designed with the following characteristics: tractor propeller, high-wing, conventional tail type, tricycle-type non-retractable landing gear, metallic structure, two reciprocating engines, simple flap, blended winglets and non-pressurized cabin. Aiming to reduce the amount spent on fuel, it was proposed to design a wingtip device (blended winglet type) optimized for the aircraft's standard operations (typical range of 800 km, cruise altitude between 8000 ft and 12000 ft).

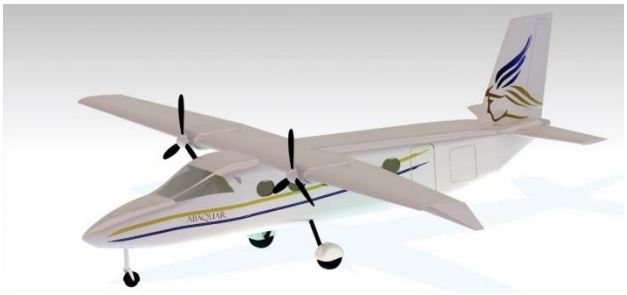

Fig. 1 – The aircraft ABQ11

When using a wingtip device the total drag of the aircraft is reduced, therefore is possible to operate at a lower power, resulting in reduction of fuel consumption and an increase of maximum range, among other benefits.

1.1 Evolution of wingtip devices technology

The Endplate Theory was the first study in the aeronautical field to propose the use of wingtip devices in order to minimize the wingtip vortex, and consequently the induced drag. It emerged in 1887 and was patented by the British scientist Fredrick W. Lanchester. However, in spite of reducing induced drag, it was not possible to obtain a complete reduction of the drag of an aircraft, since the increase of viscous drag by the use of the wingtip plate device exceeded the reduction of induced drag to the cruise condition. In July 1976, Dr. Whitcomb [1] conducted a study at the NASA Research Center in Langley and developed the concept of technology that is currently used in modern aircraft, the winglets. According to Whitcomb, the winglet could be studied as a small vertical wing that starts from the tip of the wing in order to reduce the total drag of the aircraft. In this study, a reduction of up to 20% in the induced drag with the use of winglets when compared to

a baseline wing was obtained. In 1977, Heyson [2] conducted an experiment to study the advantages of Whitcomb's winglet. The results indicated the winglets could reduce the induced drag more than the tip extension and as the winglet cant angle approached to 90°, higher was its efficiency. In early 1980, RT Jones analyzed these winglets in order to determine their effect on induced drag using Trefftz-Plane theory and concluded that the vertical length of the winglet should be twice of the horizontal length for this model to be more efficient than the extension of the wingtip [3].

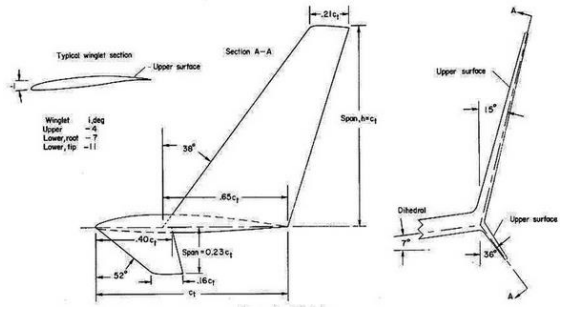

Fig. 2 – Whitcomb Winglet [1]

In 1994, Aviation Partners Inc. (API) [4] developed the concept of blended winglet, which aims to reduce interference drag in the transition from wingtip to winglets, as seen in Whitcomb model. In this wingtip device the airfoil used is generally from the same family of the wing airfoils, facilitating constructive and structural aircraft issues. Aviation Partners Boeing announced that it has saved more than 2 billion gallons of fuel in 2010. APB also reiterated that winglets could save 5 billion gallons of fuel by 2014, representing a large reduction in carbon emissions. In practice, the blended winglet demonstrated a 5% to 7% increase in the range of the Boeing 737.

Louis B. Gratzer [5] who patented the concept of blended winglet also developed the concept of the spiroid wingtip type in 1992. One side of the spiroid is connected at the leading edge of the wing while the other side is connected to the trailing edge. This device was developed with the purpose of reducing both induced drag and external noise associated with the wingtip vortex. In 1993, the API did an in-flight test with Gulfstream II achieving a 10% reduction in consumption during the cruise phase. Another study carried out with the spiroid wingtip indicated that with this device it would be possible to disperse the wingtip vortex faster, which would decrease the waiting time for landing and takeoff between one aircraft and another [6].

In 1996, the wing-grid concept was developed as a parallel multi-winglet structure proving to be efficient only for flight regime above Mach 0.7 [7]. Wing-grid generates small vortices that dissipate the energy of the main vortex, modifying the distribution of the lift and reducing the induced drag. Its main limitation is the adaptation during the different flight phases. Considering the limitation of the parallel multi-winglets, Hernan Dario Ceron et al [8] analyzed experimentally, through wind-tunnel tests, the aerodynamic characteristics of an adaptive multi-winglets system. The model consists of three winglets capable of being rotated individually in relation to the plane of the wing, as shown in Fig. 3. With this adaptive system, it was possible to increase up to 5% the maximum range.

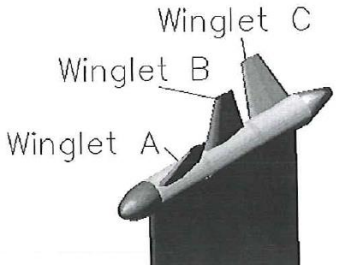

Fig. 3 – Multi-winglets system [8]

Raked wingtips and Sharklets are the latest innovation designed for Boeing 777 Family and A320, respectively. They are responsible for a reduction of 1.3 million gallons of fuel per year and 700 tons of carbon per aircraft in a year.

Despite of the good results achieved by the different type of winglet, the work here presented analyzed the blended winglet type, due the limitation to simulate different models using a VLM code.

2 Methodology

In order to reduce the operational costs by reducing the fuel consumption, the possibility of using a wingtip device was considered as an

alternative for minimizing the induced drag of the aircraft. Due to the low cruising speeds and the small aspect ratio, an aircraft flying with CL = 0.5 has a relatively high value of lift coefficient for the cruise phase, resulting in an induced drag also considerable. The only device tested was the winglet since better references are found as well as more valid approximations. Thus, the winglet is considered to modify the induced aspect ratio by 15% for a low aspect ratio wing and k_{wt}= 2.13 as specified by Equation (1) [9].

$$\frac{AR_{eff}}{AR} = \left(1 + \frac{2}{k_{wl}}\frac{h}{b}\right)^2 \qquad (1)$$

A preliminary analysis was done by varying the speed and searching for the points where the drag of the configuration with winglet exceeds the drag without winglet. The structural weight of the device and the friction and induced drag of the aircraft were considered for the calculation. Using this initial result it was possible to observe that the configuration with winglet only has greater drag for speeds 50% above the cruising speed. At the cruising speed, there is a smaller total drag with the use of winglet. Still, for the take-off situation, the total drag is 11% lower than the configuration without a tip device. Based on these preliminary analyzes the possibility of increasing the aircraft efficiency was detected using an optimized wingtip devices. Thus, an MDO implemented in Matlab® [10] was developed to analyze the influence of four parameters of a blended winglet: cant angle, winglet span, taper ratio and sweep angle (Fig. 4 and Fig. 5).

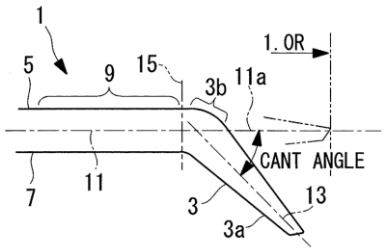

Fig. 4 – Winglet cant angle definition

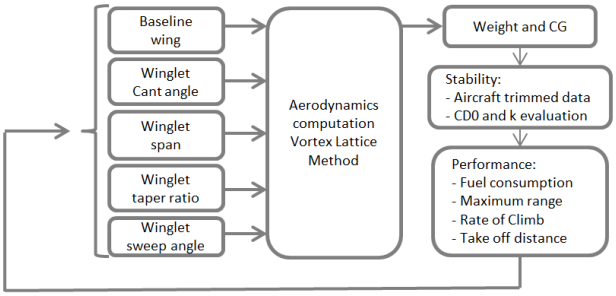

Fig. 5 – Winglet MDO flow chart

The method was based on the Trefftz-Plane theory for the calculation of induced drag, applied in a classical model of Vortex Lattice Method, available in an open-source software called Tornado VLM [11] with a discretized mesh in the chordwise direction and in the spanwise direction (Fig. 6) [12][13].

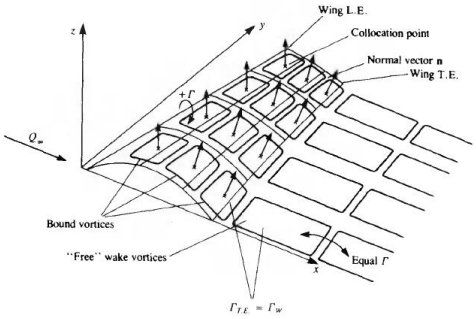

Fig. 6 – Classical VLM Mesh distribution

The drag value (CD_0) of the aircraft components were calculated using the equations presented in Raymer [14], Perkins [15] and Torenbeek [16]. The induced drag factor (k) was obtained through the VLM code, considering a linear interpolation of CD and CL^2, as presented in Equation (2).

$$CD = CD0 + k * CL^2 \qquad (2)$$

To evaluate the aircraft performance data, the equations described in Raymer [14] and Perkins [15] were used. To achieve the results, it was necessary to estimate the aircraft empty weight, using analytical methods [14], but considering the wing load distribution, obtained by the software XFLR5 [13].

3 Results

To achieve the best winglet solution, through the methodology described in section 2, an analysis was carried out in four phases: convergence of the MDO, first iteration, refined iteration and comparison between baseline wing and the baseline wing with the final winglet. Table 1 presents the ABQ11 aircraft baseline wing data before the optimization process:

Table 1 – Baseline wing data

	Parameters	Value
Main data	Wing span (b) [m]	14.78
	Wing area (S) [m²]	23
	Mean Aerodynamic chord [m]	1.59
	Wing Aspect Ratio (AR)	9.5
	Sweep angle at ¼ of the chord [°]	0
Section 0 (Root)	Airfoil	NACA 23018
	Section chord [m]	1.74
	Section span position [m]	0
	Taper ratio [-]	1.00
	Twist [°]	0
Section 1	Airfoil	NACA 23015
	Section chord [m]	1.74
	Section span position [m]	3.00
	Taper ratio	1.00
	Twist[°]	0
Section 2 (Tip)	Airfoil	NACA 23012
	Section chord [m]	1.13
	Section span position [m]	7.39
	Taper ratio [-]	0.65
	Twist [°]	0

3.1 MDO convergence analysis

A convergence analysis was carried out to determine the VLM mesh size for the evaluation of CL and CD wing coefficients. It was considered as a reasonable mesh the one which values of CL vary by 10^{-3} and CD values vary by $5x10^{-4}$. It can be seen from Fig. 7 that the mesh with 60 panels (half-wing) presented a satisfactory result within the requirement.

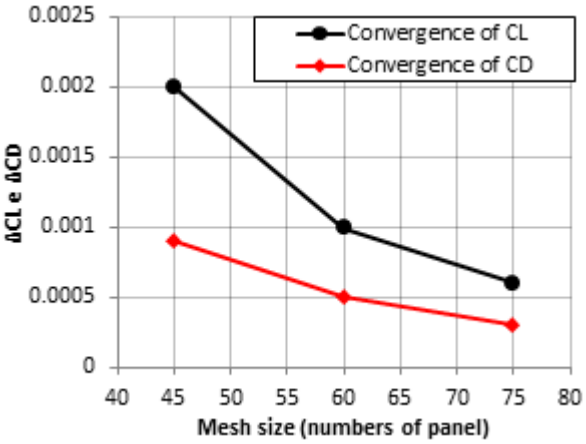

Fig. 7 – VLM mesh size convergence

3.2 First Iteration

The first iteration was performed with a mesh containing 60 panels, totalizing 3024 runs. The winglet parameters were varied as follows:

- Cant Angle [deg]: 90, 80, 70, 60, 50, 40, 30, 20, 10, 0, -10, -20, -30, -40, -50, -60, -70, -80 e -90;
- Span [m]: 0.10, 0.15, 0.20, 0.25, 0.30, 0.35 e 0.40;
- Taper ratio [-]: 0.2, 0.3, 0.4, 0.5, 0.6 e 0.7;
- Sweep angle at ¼ of the chord [deg]: 30, 40, 50 e 60.

3.2.1 Influence of winglet cant angle

In order to understand the influence of the cant angle parameter, it was plotted all results in function of it. Through the Fig. 8 and Fig. 9 it was possible to conclude that the winglets with cant angle between -50° and -60° presented the lowest fuel consumption and the highest maximum range.

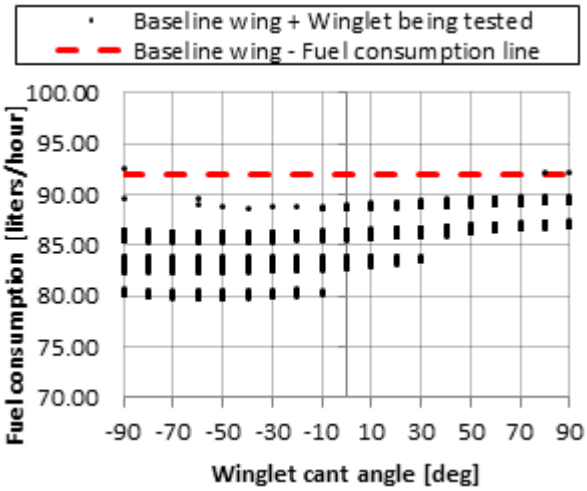

Fig. 8 – Influence of cant angle on fuel consumption

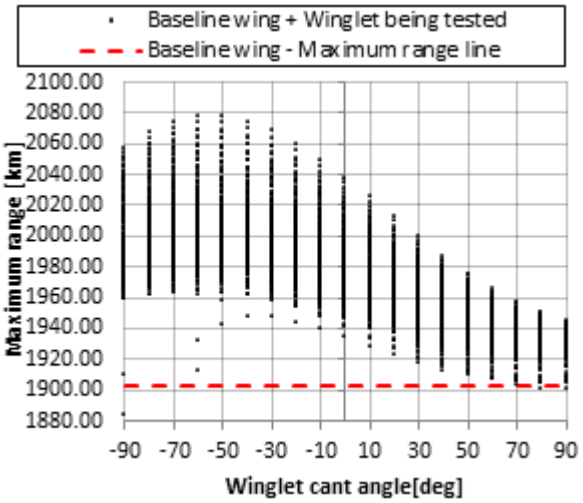

Fig. 9 – Influence of cant angle on maximum range

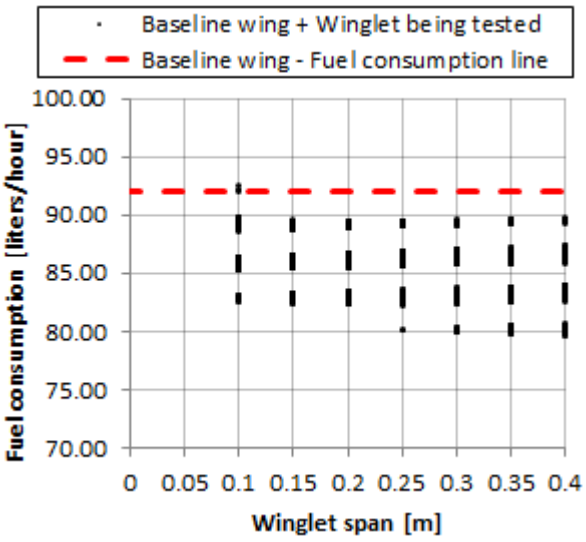

Fig. 10 – Influence of winglet span on fuel consumption

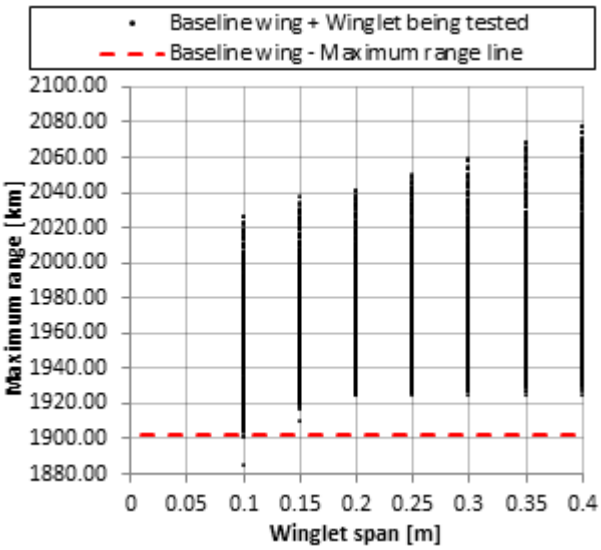

Fig. 11 – Influence of winglet span on maximum range

3.2.2 Influence of winglet span

Despite the increase in CD_0 (viscous drag) due the increment in the wetted area, it was observed that the maximum range is directly proportional to the winglet span (Fig. 11). This fact is due the reduction of k factor (induced drag) related with the gain of the wing effective Aspect Ratio.

3.2.3 Influence of winglet taper ratio

The taper ratio parameter did not present a direct relation with the fuel consumption. For a same taper ratio, other parameters have more influence, causing a wide range of results. When tapering the winglet with other values, the amplitude of results does not have a considerable variation, which corroborates the fact mentioned above. Even though, it is possible to see that the taper ratio value of 0.2 presented the best result (Fig. 12 and Fig. 13).

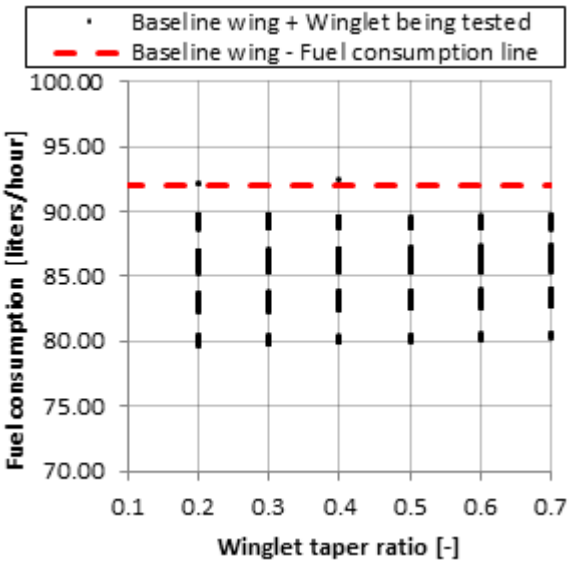

Fig. 12 – Influence of winglet taper ratio on fuel consumption

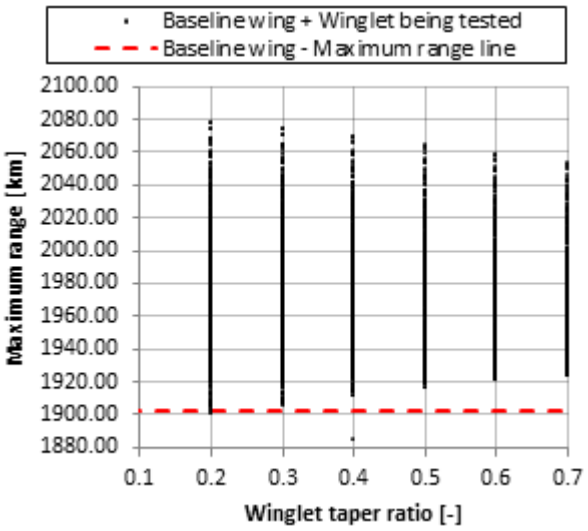

Fig. 13 – Influence of winglet taper ratio on maximum range

3.2.4 Influence of winglet sweep angle

Unlike the taper ratio parameter, it was identified through the Fig. 14 and Fig. 15 that the sweep angle is directly related to induced drag. The bigger the sweep angle, the lower the fuel consumption and the higher the maximum range.

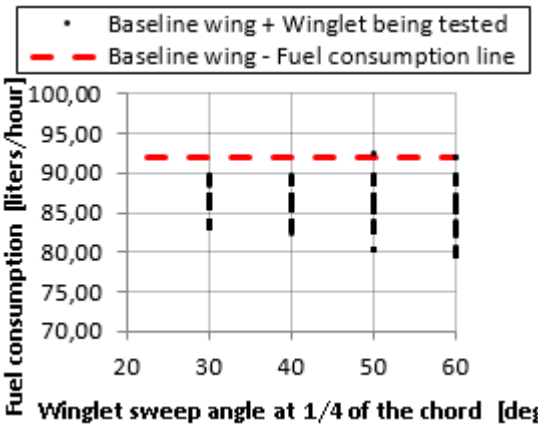

Fig. 14 – Influence of winglet sweep angle on fuel consumption

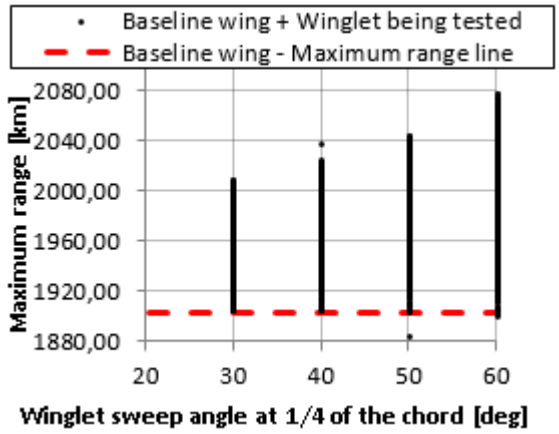

Fig. 15 – Influence of winglet sweep angle on maximum range

3.2.4 First Iteration results

After this first analysis, it was selected two winglets as candidate for the optimum solution, as shown in Table 2.

Table 2 – First iteration results comparison

	BASELINE WING	WINGLET 1	WINGLET 2
Cant Angle [°]	-	-50	-60
Winglet span [m]	-	0.4	0.4
Taper ratio [-]	-	0.2	0.2
Sweep angle at ¼ of the chord [deg]	-	60	60
CD0	0.0283	0.0286	0.0286
k	0.0383	0.0311	0.0311
Fuel consumption [liters/hour]	91.95	79.69	79.69
Maximum range[Km]	1902.51	2077.40	2077.34

3.3 Refined Iteration

With the results of the first analysis, it was performed a new iteration, refining the parameters between Winglet 1 and Winglet 2. The only exception was the winglet span, which was explored more solutions beyond the 0.4 m, but with a maximum value of 0.8 m, due geometric constraints. The following parameters were tested:

- Cant angle [deg]: 50, -55 e -60;
- Span [m]: 0.4, 0.5, 0.6, 0.7 e 0.8;
- Taper ratio [-]: 0.2;
- Sweep angle at ¼ of the chord [deg]: 60.

Through the Fig. 16 and Fig. 17, it can be seen that the best solution is the one with a cant angle (negative) of -50 degrees.

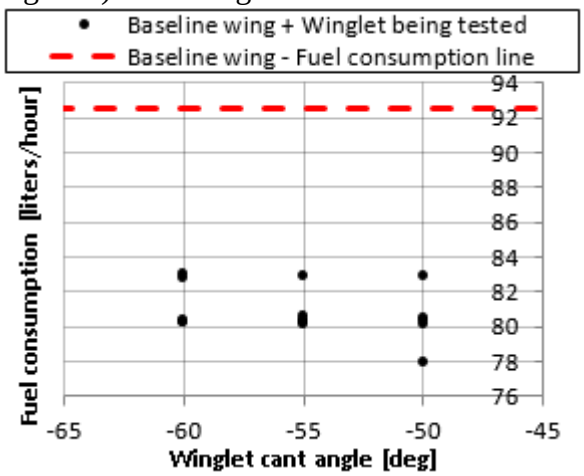

Fig. 16 – Influence of cant angle on fuel consumption (refined iteration)

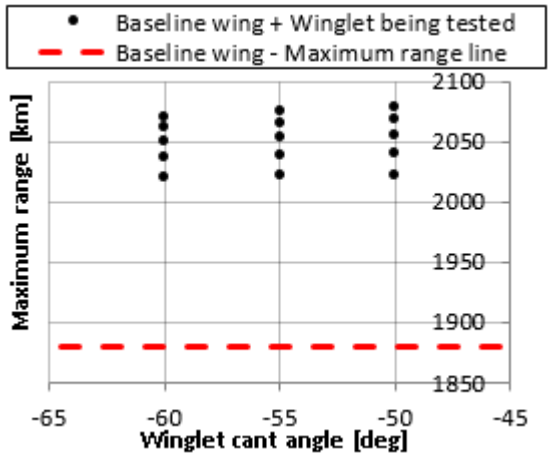

Fig. 17 – Influence of cant angle on maximum range (refined iteration)

Regarding the winglet span parameter, it was observed that the efficiency of the wingtip device was increased by the span increment, enabling a gain in maximum range and a reduction in total consumption.

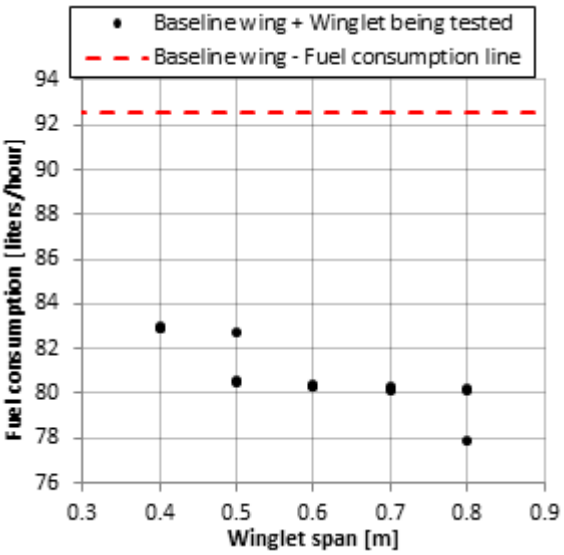

Fig. 18 – Influence of winglet span on fuel consumption (refined iteration)

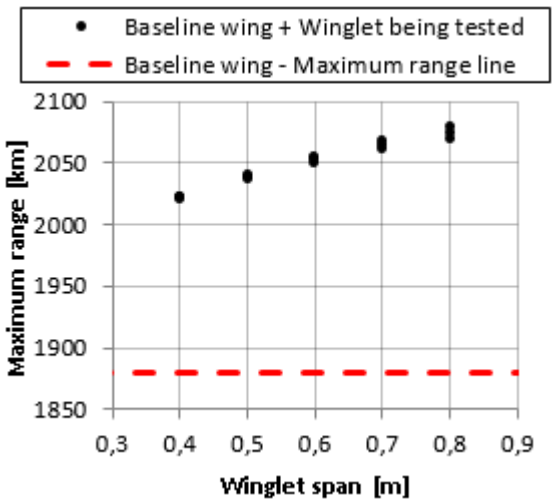

Fig. 19 – Influence of winglet span on maximum range (refined iteration)

After these iterations, it was chosen to use the device that presented the best performance in all the tests and still with a restriction of having the maximum size of 80 cm according to the requirement. The values of the final winglet are presented in the Table 3.

Table 3 – Final winglet data

	BASELINE WING	Final WINGLET
Cant Angle [°]	-	-50
Winglet span [m]	-	0.8
Taper ratio [-]	-	0.2
Sweep angle at ¼ of the chord [deg]	-	60
CD0	0.0283	0.0288
k	0.0383	0.0307
Fuel consumption [liters/hour]	92.52	77.91
Maximum range[Km]	1879.07	2078.77

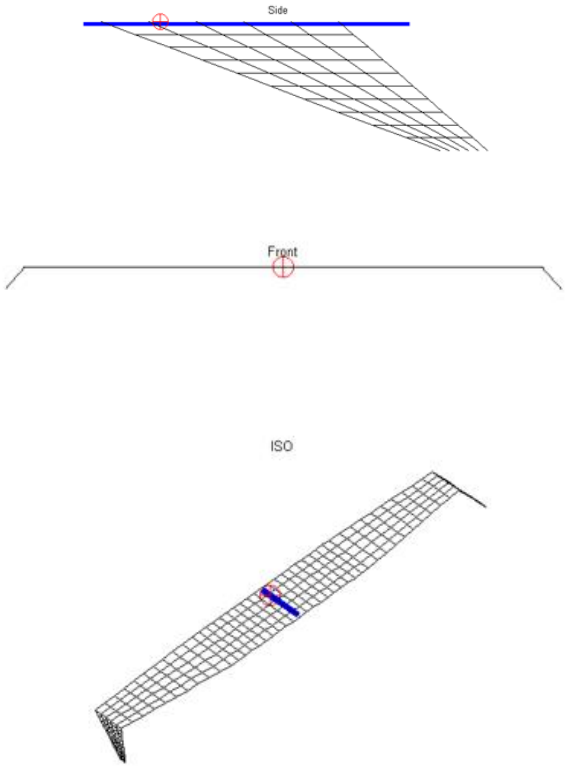

Fig. 20 – Final winglet geometry

3.4 Comparison between baseline wing and baseline wing with the final winglet

In order to understand the effect of the final winglet on the wing loading, it was made a comparison between the baseline wing and the baseline wing with the final winglet in a cruise condition (altitude of 8000 ft and true airspeed of 74 m/s). Using the classical Vortex Lattice Method it is possible to observe that the wing with the final winglet presents a greater load on the tip (Fig. 21), which increases the lift, however a wing with a loaded tip can be a problem during a stall, presenting a loss in lateral control during the recovery.

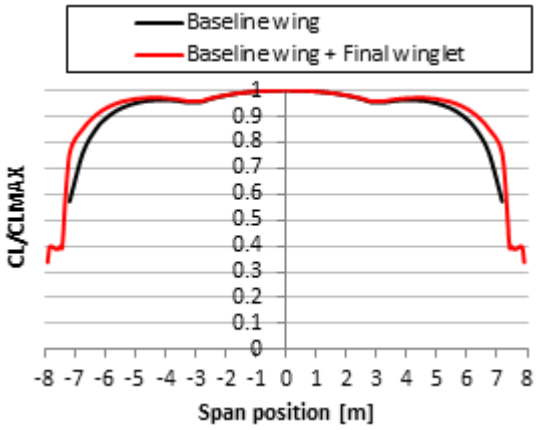

Fig. 21 – Local CL coefficient comparison

Thus, a stall progression analysis was performed to verify if the stall would affect the aileron commands during the recovery. The separation point is interpolated according to the thickness of the airfoil and the local angle of attack through a second-order polynomial equation with maximum separation limited at the trailing edge. For the baseline wing, it is possible to conclude that the stall starts at the wing root and propagates to the tip region (Fig. 22). Also, the ailerons are not affected at the beginning of the stall, allowing the aircraft to use the lateral control to recovery from a non-safety condition.

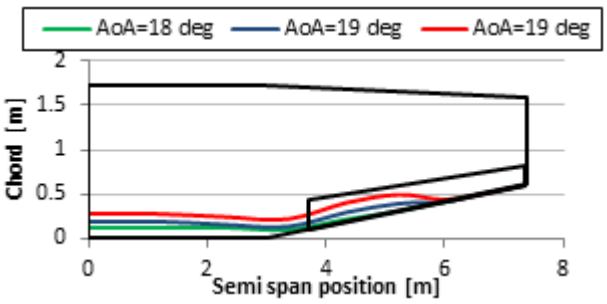

Fig. 22 – Stall progression of Baseline wing

For the wing with the final winglet installed, the same result was achieved. It is possible to notice

that the stall still begins in the root region propagating towards the tip, however a greater area of the aileron is affected by the increase of the load of the tip caused by the winglets (Fig. 23). Even so, it is concluded that the aircraft still has safe conditions, because at the beginning of the stall it is still possible to command the aircraft avoiding a possible spin maneuver.

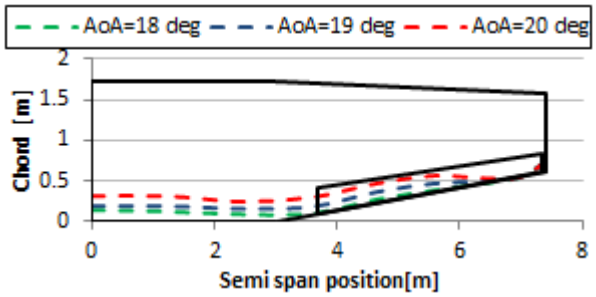

Fig. 23 – Stall progression of Baseline wing with the final winglet

To conclude the aerodynamic comparison, a drag breakdown is presented for the ABQ11 in a cruise condition. It is possible to observe (Fig. 24) that even with the increase of CD_0, caused by the winglet wetted area increment; there is a reduction of the total drag, because of the induced drag value decrease.

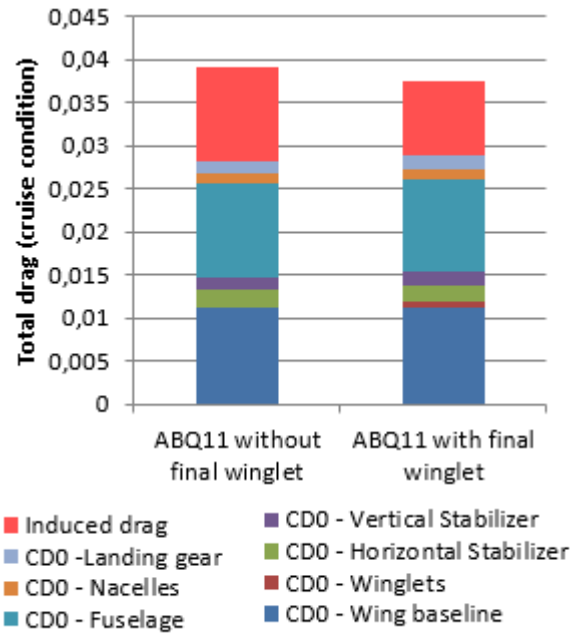

Fig. 24 – Drag breakdown comparison – cruise condition

Finally, a comparative table is presented (Table 4) summarizing all the results to better understand the final gain obtained by the optimization process described in this work.

Table 4 – Comparative table

Parameter	ABQ11 without final winglet	ABQ11 with final winglet
CD_0	0.0283	0.0288
k	0.0383	0.0307
Fuel consumption	92 [liters/hour]	78 [liters/ hour]
Maximum range	1878 km	2078 km
Cruise speed	79 m/s	74 m/s
$C_{L\ CRUISE}$	0.49	0.56
$\alpha_{\ CRUISE}$	4.5 [°]	5.5 [°]
Speed of maximum Rate of Climb	41 m/s	45 m/s
Maximum Rate of Climb	1790 ft/min	1900 ft/min
Maximum efficiency (L/D)	15.1	16.8
Take off distance	1211 m	1195 m
Maximum bending moment	$36.8*10^4$ N.m	$42.2*10^4$N.m
Maximum shear force	$11.8*10^4$ N	$12.6*10^4$ N
Wing weight	259.9 kg	298.1 kg

The main advantages of the Baseline wing with the final winglet are:

- Reduction of fuel consumption by 14 liters/hour
- Increase of maximum range by 200 km
- 110 ft/min gain in Rate of Climb (ROC)
- Increase of maximum efficiency (L/D) from 15.1 to 16.8

The main disadvantages are:

- Increase of maximum bending moment by 15%
- Increase of maximum shear force by 7%
- Increase of the structural wing weight from 259.9 kg to 298.1 kg

4 Conclusions

From the motivation related to the reduction of operational costs of a commuter aircraft design up to 11 passengers, a brief description of the problem involving the induced drag was made. Using computer-implemented aerodynamic (VLM) models, it was possible to develop a multidisciplinary optimization method to verify the influence of winglets geometry in aerodynamics, loads, stability, weight and performance of the aircraft.

It was observed that negative values of cant angle presented better results, both in the reduction of fuel consumption and in the increase of the range. For taper ratio, an optimum value of 0.2 was reached. For the winglet span it has been realized that the dimension aiming the reduction of fuel consumption is 80 cm in length. Finally, it was concluded that the sweep angle of 60° presented satisfactory results within the stipulated requirements. A detailed comparison was made involving aeronautical areas, such as aerodynamics, weight, loads and performance; presenting the advantages and disadvantages of using the wingtip device.

When using the final winglet there is a 15% reduction in fuel consumption, which represents an annual reduction of US$ 120,000 per aircraft only in fuel costs. These values corroborate the motivation of this work, leading to the conclusion that the multidisciplinary design of the blended winglet fulfilled its main goal with success, allowing the ABQ11 aircraft the lowest operating cost of its category.

5 References

[1] R. T. Whitcomb, *"A Design Approach and Selected Wing-Tunnel Result at High Subsonic Speed for Wing-Tip Mounted Winglets"*, NASA TN D-8260, 1976.

[2] e. a. H. H. Heyson, *"Theoretical Parametric Study of the Relative Advantages of Winglets and Wing-tip Extension,"* NASA Langely Research Centre, Virginia1977.

[3] R. T. Jones and T. A. Lasinski, *"Effect of Winglets on the Induced Drag of Ideal Wing Shapes,"* NASA TM-81230, 1980.

[4] L. B. Gratzer, *"Blended winglet,"* ed: Google Patents, 1994.

[5] L. B. Gratzer, *"Spiroid-tipped wing,"* ed: Google Patents, 1992.

[6] e. a. J. E. Guerrero, *"Biomimetic spiroid winglets for lift and drag control,"* Comptes Rendus Mécanique, vol. 340, pp. 67-80, 2012.

[7] U. La Roche, *"Wing with a wing grid as the end section,"* ed: Google Patents, 1998.

[8] H. D. Cerón Muñoz, *Análise experimental das características aerodinâmicas de multi-winglets adaptativas*. Diss. Universidade de São Paulo.

[9] I. Kroo, *Aircraft Design: Synthesis and Analysis*, http://adg.stanford.edu/aa241/AircraftDesign.html (15/06/2015), 2001

[10] M. U. Guide, *"The mathworks."* Inc., Natick, MA 5 (1998): 333.

[11] T. Melin, *"A vortex lattice MATLAB implementation for linear aerodynamic wing applications."* Master's Thesis, Department of Aeronautics, Royal Institute of Technology (KTH), Stockholm, Sweden (2000).

[12] J. Katz e A. Plotkin, *Low-Speed Aerodynamics*, Cambridge University Press, 2001.

[13] A. Deperrois, *"XFLR5 Analysis of foils and wings operating at low reynolds numbers."* Guidelines for XFLR5 (2009).

[14] D. P. Raymer, Aircraft Design: *A Conceptual to Approach*, AIAA, 1992.

[15] C. Perkins, *Airplane Performance Stability and Control*, Central Book Company, 1970.

[16] E. Torenbeek, *Synthesis of Subsonic Airplane Design: An Introduction to the Preliminary Design of Subsonic General Aviation and Transport Aircraft, with Emphasis on Layout, Aerodynamic Design, Propulsion and Performance*, Springer, 1982.

6 Contact Author Email Address

Joabe Marcos de Souza: joabemsouza@gmail.com
Fernando Martini Catalano: catalano@sc.usp.br

7 Copyright Statement